uPAR induces epithelial–mesenchymal transition in hypoxic breast cancer cells

Robin D. Lester, Minji Jo, Valérie Montel, Shinako Takimoto, and Steven L. Gonias

Department of Pathology, University of California, San Diego, La Jolla, CA 92093

Hypoxia activates genetic programs that facilitate cell survival; however, in cancer, it may promote invasion and metastasis. In this study, we show that breast cancer cells cultured in 1.0% O_2 demonstrate changes consistent with epithelial–mesenchymal transition (EMT). Snail translocates to the nucleus, and E-cadherin is lost from plasma membranes. Vimentin expression, cell migration, Matrigel invasion, and collagen remodeling are increased. Hypoxia-induced EMT is accompanied by increased expression of the urokinase-type plasminogen activator receptor (uPAR) and activation of cell signaling factors downstream of uPAR, including Akt and Rac1. Glycogen synthase kinase-3β is phosphorylated, and Snail expression is increased. Hypoxia-induced EMT is blocked by uPAR gene silencing and mimicked by uPAR overexpression in normoxia. Antagonizing Rac1 or phosphatidylinositol 3-kinase also inhibits development of cellular properties associated with EMT in hypoxia. Breast cancer cells implanted on chick chorioallantoic membranes and treated with $CoCl_2$, to model hypoxia, demonstrate increased dissemination. We conclude that in hypoxia, uPAR activates diverse cell signaling pathways that cooperatively induce EMT and may promote cancer metastasis.

Introduction

Hypoxia is a hallmark of diverse human malignancies, including breast cancer, head and neck cancer, prostate cancer, pancreatic cancer, brain tumors, and malignant melanoma (Harrison and Blackwell, 2004). The extent of hypoxia in a tumor may represent an independent indicator of poor prognosis (Chia et al., 2001); however, the mechanisms by which hypoxia affects cancer progression remain incompletely understood. Under decreased O_2 tension, the transcription factor, hypoxia-inducible factor 1α (HIF-1α), is stabilized. HIF-1α dimerizes with HIF-1β to activate a complex genetic program that is responsible for many hypoxia-associated changes in cell physiology, including expression of vascular endothelial growth factor (VEGF) and induction of angiogenesis (Forsythe et al., 1996). Constitutive expression of HIF-1α renders tumor cells resistant to hypoxia and/or nutrient deprivation (Akakura et al., 2001). Thus, clonal selection of HIF-1α–overexpressing cells may increase the likelihood that tumor cells survive at implantation sites during metastasis (Vaupel and Harrison, 2004).

In hypoxic cancer cells, cell signaling pathways that support invasion and metastasis may be activated downstream of the hepatocyte growth factor receptor/c-Met (Pennacchietti et al., 2003) or the erythropoietin receptor (EpoR; Leyland-Jones, 2003; Lester et al., 2005). Hypoxia also may induce expression of the urokinase-type plasminogen activator (uPA) receptor (uPAR; Graham et al., 1999; Rofstad et al., 2002). In breast cancer, uPAR expression is associated with a poor prognosis (Del Vecchio et al., 1993; Bianchi et al., 1994; de Vries et al., 1994). uPAR may promote cancer progression by multiple mechanisms (Ossowski and Aguirre-Ghiso, 2000; Blasi and Carmeliet, 2002). By binding uPA at the leading edge of the migrating cell, uPAR organizes a cascade of extracellular proteases that facilitate cellular penetration of tissue boundaries (Andreasen et al., 1997). uPAR also laterally associates with integrins in the plasma membrane, regulating the state of integrin activation (Wei et al., 1996, 2001; Blasi and Carmeliet, 2002). Furthermore, uPAR functions in association with coreceptors, including integrins, receptor tyrosine kinases, and G protein–coupled receptors, to initiate signal transduction (Nguyen et al., 1999; Liu et al., 2002; Resnati et al., 2002; Jo et al., 2003; Kiyan et al., 2005).

uPAR-dependent cell signaling is regulated by ligands. Binding of uPA to uPAR activates FAK, c-Src, H-Ras, Akt, extracellular signal-regulated kinase (ERK)/MAPK, and myosin light chain kinase (Nguyen et al., 1999; Chandrasekar et al.,

R.D. Lester and M. Jo contributed equally to this paper.

Correspondence to Steven L. Gonias sgonias@ucsd.edu

Abbreviations used in this paper: CAM, chorioallantoic membrane; DN, dominant-negative; EMT, epithelial–mesenchymal transition; EpoR, erythropoietin receptor; ERK, extracellular signal-regulated kinase; GSK-3β, glycogen synthase kinase-3β; HIF, hypoxia-inducible factor; HPRT-1, hypoxanthine phosphoribosyltransferase 1; PI3K, phosphatidylinositol 3-kinase; qPCR, quantitative PCR; sh, short hairpin; uPA, urokinase-type plasminogen activator; uPAR, uPA receptor; VEGF, vascular endothelial growth factor.

The Journal of Cell Biology, Vol. 178, No. 3, July 30, 2007 425–436
http://www.jcb.org/cgi/doi/10.1083/jcb.200701092

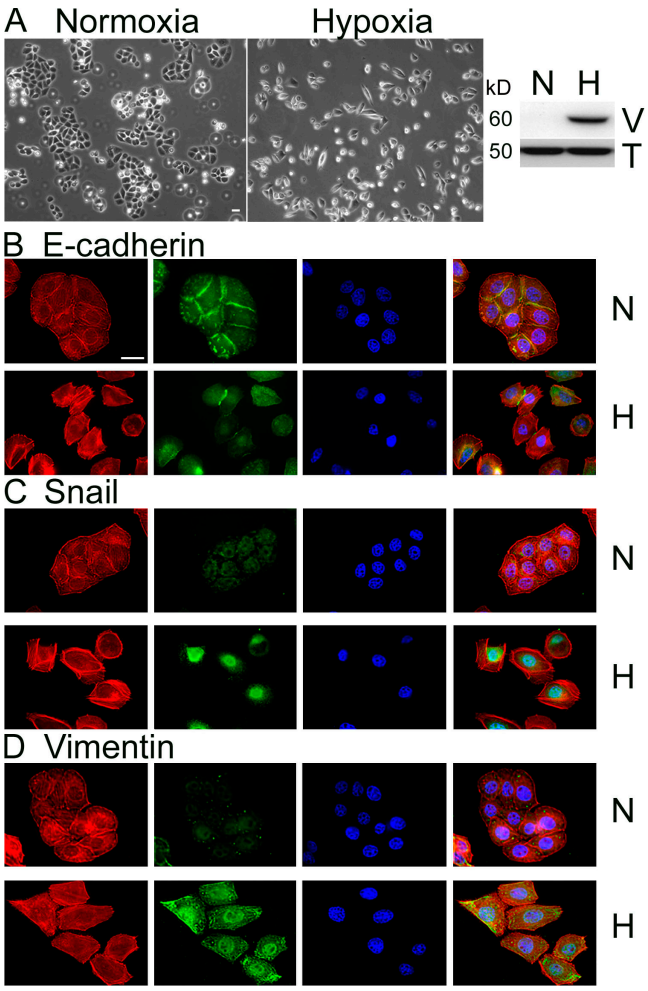

Figure 1. **Hypoxia induces EMT in MDA-MB-468 cells.** (A) Cells were cultured for 50 h in 21% O_2 (normoxia; N) or 1.0% O_2 (hypoxia; H). Cell images were captured by phase-contrast microscopy. Cell extracts were subjected to SDS-PAGE and immunoblot analysis to detect vimentin (V), and tubulin (T). (B–D) Cells that were incubated for 50 h in 21% O_2 (N) or 1.0% O_2 (H) were immunostained to detect E-cadherin (B), Snail (C), or vimentin (D), in the green channel, with phalloidin (red), and with DAPI (blue). Bar, 50 μm.

2003; Alfano et al., 2006; Monaghan-Benson and McKeown-Longo, 2006). uPAR also binds directly to vitronectin, and this interaction promotes activation of Rac1 (Kjoller and Hall, 2001; Ma et al., 2002). A second mechanism by which uPAR controls Rac1 activation is by regulating the interaction of $\alpha_5\beta_1$ with fibronectin (Wei et al., 2006). These uPAR-dependent cell signaling events impact cell migration and survival (Ossowski and Aguirre-Ghiso, 2000; Blasi and Carmeliet, 2002); however, the role of uPAR-initiated cell signaling in cell physiology remains incompletely understood.

Zhang et al. (2003) demonstrated that in kidney epithelial cells, α3 integrins and uPAR cooperate to induce phenotypic changes consistent with epithelial–mesenchymal transition (EMT). In cancer, EMT may be an important step leading to invasion and metastasis (Thompson et al., 2005). At the molecular level, EMT is characterized by loss of epithelial cell markers, including the cell adhesion protein, E-cadherin (Thiery, 2002), and acquisition of mesenchymal markers, such as vimentin (Grunert et al., 2003). A major mechanism by which E-cadherin is down-regulated in EMT is transcriptional repression by Snail (Nieto, 2002). Overexpression of Snail is sufficient to induce EMT and is associated with highly invasive tumors both in mice and humans (Cano et al., 2000). In ovarian cancer cells, tumor hypoxia increases Snail levels and decreases E-cadherin expression (Imai et al., 2003). Absence of the von Hippel–Landau tumor suppressor in renal carcinoma cells increases the level of HIF-1α and is associated with decreased expression of E-cadherin (Krishnamachary et al., 2003). These studies suggest a relationship between tumor hypoxia and EMT. Our objective was to further elucidate this linkage.

In this study, we demonstrate that hypoxia induces diverse molecular, phenotypic, and functional changes in breast cancer cells that are consistent with EMT. We also show that cell signaling factors, which are thought to be involved in EMT, are activated in hypoxic cancer cells, including ERK/MAPK, Rac1, Akt, and glycogen synthase kinase-3β (GSK-3β). The EMT-associated phenotypic changes and changes in cell signaling are due to hypoxia-induced uPAR expression and activation of uPAR-dependent cell signaling. Hypoxia-induced EMT is blocked by uPAR gene silencing and mimicked by uPAR overexpression in normoxia. Using a newly developed chick chorioallantoic membrane (CAM) model system, we show that hypoxic conditions promote cancer cell dissemination in vivo. We conclude that EMT may be induced in hypoxic cancer cells, by a mechanism that involves activation of uPAR-dependent cell signaling.

Results

MDA-MB-468 cells undergo EMT in hypoxia

The concentration of O_2 in conventional cell culture is 21%, corresponding to a PO_2 of 150 mm Hg, well above the PO_2 of well-perfused tissues in vivo (40 mm Hg; Semenza, 2001). To better model the tumor microenvironment, particularly at the hypoxic core, we cultured breast cancer cells in an incubator adjusted to 1.0% O_2. Fig. 1 A shows that after 50 h in hypoxia, MDA-MB-468 cells, which typically appear epithelial with well-developed cell junctions, acquire a spindle shape and generally lose cell contacts. Immunoblot analysis shows that MDA-MB-468 cells express vimentin when cultured in 1.0% O_2.

EMT has been defined as a three-part process in which cells acquire a fibroblast-like morphology, down-regulate epithelial-specific proteins such as E-cadherin while simultaneously expressing mesenchymal proteins such as vimentin, and ultimately, digest and migrate through ECM (Grunert et al., 2003). To further test whether the morphologic changes in hypoxic MDA-MB-468 cells represent EMT, we performed immunofluorescence microscopy, examining the epithelial cell marker E-cadherin. As shown in Fig. 1 B, after 50 h at 1.0% O_2, E-cadherin was lost from the cell surface in most cells. Residual E-cadherin remained localized primarily in intracellular pools.

Localization of the transcription factor, Snail, was examined by costaining cells with DAPI. Under normoxic cell culture conditions (21% O_2), immunostaining for Snail was localized diffusely throughout the cytoplasm (Fig. 1 C). In contrast,

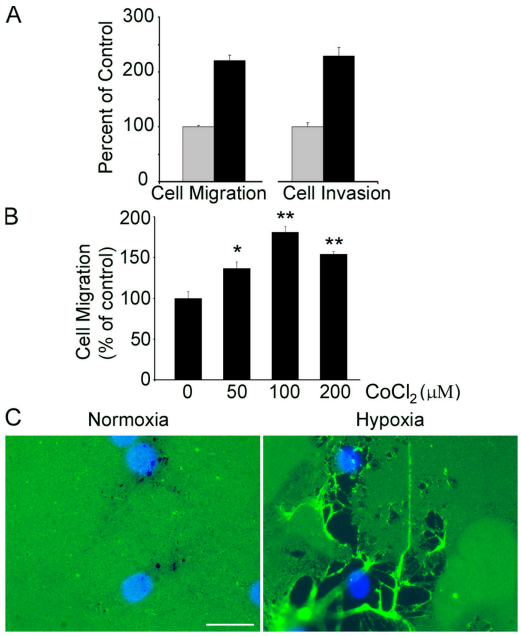

Figure 2. **Hypoxia promotes cell migration, invasion, and collagen remodeling.** (A) MDA-MB-468 cells were added to Transwell chambers, in which the membranes were precoated with FBS (cell migration; $n = 21$) or in which reconstituted Matrigel was present (cell invasion; $n = 10$). Studies were performed for 24 h in 21% O_2 (gray bar) or 1.0% O_2 (black bar). Migration and invasion are expressed relative to the levels observed with normoxic controls (mean ± SEM). (B) MDA-MB-468 cells were treated with $CoCl_2$ or with vehicle. Cells were allowed to migrate for 24 h. Cell migration is expressed relative to that observed with vehicle (mean ± SEM; $n = 3$). *, $P < 0.05$; **, $P < 0.005$. (C) Cells were cultured for 18 h on fluorescein-labeled type I collagen in 21% (normoxia) or 1.0% O_2 (hypoxia). Type I collagen remodeling was assessed. Cell nuclei are stained with DAPI. Bar, 50 μm.

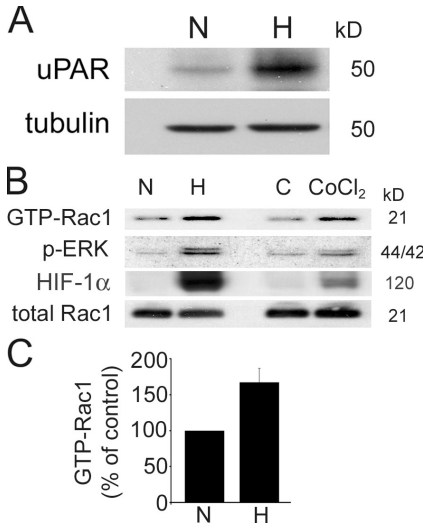

Figure 3. **Hypoxia increases uPAR levels and activates cell signaling factors known to be downstream of uPAR.** (A) MDA-MB-468 cells were cultured for 24 h in 21% O_2 (N) or 1.0% O_2 (H). Cell extracts were subjected to SDS-PAGE and immunoblot analysis to detect human uPAR using antibody 3932 and tubulin. (B) MDA-MB-468 cells were cultured for 15 h in 21% O_2 (N) or 1.0% O_2 (H), treated with 100 μM $CoCl_2$ or with vehicle (control; C). Cell extracts were affinity precipitated with PAK-1 PBD and subjected to immunoblot analysis to detect GTP-bound Rac1. The original cell extracts were studied by immunoblot analysis to determine total Rac1. Cell extracts were also probed for phosphorylated ERK/MAPK and HIF-1α. (C) The results of three separate experiments were averaged to determine the percentage of increase in activated Rac1 in hypoxia (mean ± SEM; $n = 3$).

in 1.0% O_2, Snail translocated to the nucleus. Fig. 1 D shows that vimentin immunostaining was substantially increased in MDA-MB-468 cells cultured in hypoxia, confirming the results of our immunoblot analyses. In control experiments, none of the described antigens were detected when primary antibody was omitted.

Hypoxia promotes cell migration, Matrigel invasion, and ECM remodeling

EMT is thought to promote cancer cell migration and invasion (Grunert et al., 2003). To study the effects of hypoxia on cell migration, we examined cells in Transwell chambers maintained in 1.0 or 21% O_2. The underside of each Transwell membrane was coated with FBS so that vitronectin was the primary protein adsorbed to the surface in a haptotactic gradient (Hayman et al., 1983). 10% FBS also was added to the bottom chamber as a chemoattractant. MDA-MB-468 cells were added to each Transwell in a single-cell suspension. As shown in Fig. 2 A, cell migration was increased 2.2 ± 0.1-fold ($P < 0.001$; $n = 21$) in 1.0% O_2. Similarly, invasion of MDA-MB-468 cells through reconstituted 3D Matrigel matrices was increased 2.3 ± 0.2-fold ($P < 0.001$; $n = 10$) in 1.0% O_2.

To confirm these results using a second experimental protocol, we treated MDA-MB-468 cells with $CoCl_2$, which stabilizes HIF-1α and mimics many of the cellular changes observed in hypoxia (Schuster et al., 1989; Wang and Semenza, 1993). 100 μM $CoCl_2$ increased MDA-MB-468 cell migration 1.8 ± 0.1-fold ($P < 0.005$; $n = 3$) compared with vehicle-treated control cultures (Fig. 2 B). These results support a model in which hypoxia-induced EMT, in MDA-MB-468 cells, is associated with more aggressive cell behavior. To further test this model, we compared the ability of MDA-MB-468 cells to remodel fluorescein-labeled type I collagen in 1.0 and 21% O_2. The collagen was adsorbed to microscope coverslips and labeled with fluorescein before adding cells. As shown in Fig. 2 C, remodeling of the fluorescent collagen was substantially increased when the coverslips were maintained in 1.0% O_2.

Signaling pathways downstream of uPAR are activated in hypoxia

We previously demonstrated that activation of EpoR-dependent cell signaling promotes migration of MCF-7 breast cancer cells in hypoxia (Lester et al., 2005). Therefore, we tested whether Epo or EpoR are up-regulated in hypoxic MDA-MB-468 cells; however, this was not the case (unpublished data). Instead, MDA-MB-468 cells demonstrated substantially increased uPAR expression, as determined by immunoblot analysis (Fig. 3 A). uPAR expression also was increased when MDA-MB-468 cells were treated with $CoCl_2$ (unpublished data). These results, taken in the context of our previous study (Lester et al., 2005), suggest that receptor activation to promote cell migration and invasion in hypoxia may occur in a cell-specific manner.

We hypothesized that activation of uPAR-dependent cell signaling may be responsible for the molecular and morphological changes observed in MDA-MB-468 cells under hypoxic

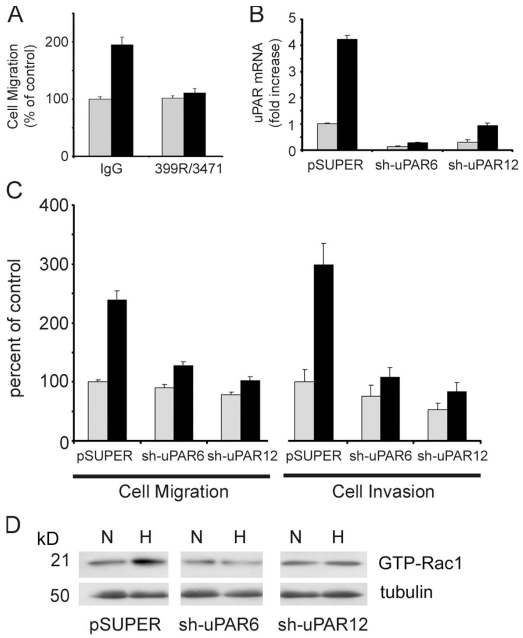

Figure 4. **uPAR is necessary for hypoxia-promoted cell migration, invasion, and Rac1 activation.** (A) MDA-MB-468 cells were pretreated with 25 μg/ml uPA-specific antibody 3471 and 25 μg/ml uPAR-specific antibody 399R or with 50 μg/ml control IgG. Cells were allowed to migrate in Transwell chambers for 24 h in 21% O_2 (gray bars) or 1.0% O_2 (black bars). Cell migration is expressed as a percentage of that observed with control IgG in normoxia (mean ± SEM; $n = 6$). (B) MDA-MB-468 cells expressing empty vector (pSUPER), sh-uPAR6 cells, and sh-uPAR12 cells were cultured for 24 h in 21% O_2 (gray bars) or 1.0% O_2 (black bars). uPAR mRNA was determined by qPCR. Results are normalized against HPRT-1 and compared with the level observed in the pSUPER cells in normoxia (mean ± SEM; $n = 3$). (C) pSUPER, sh-uPAR6, and sh-uPAR12 cells were allowed to migrate in Transwell chamber (cell migration) or to invade Matrigel (cell invasion) for 24 h in 21% O_2 (gray bars) or 1.0% O_2 (black bars). Results are expressed as a percentage of that observed with pSUPER cells in normoxia (mean ± SEM; $n = 7$ and $n = 6$, respectively). (D) pSUPER, sh-uPAR6, and sh-uPAR12 cells were cultured for 15 h in 21% O_2 (N) or in 1.0% O_2 (H). Cell extracts were affinity precipitated with PAK-1 PBD and subjected to immunoblot analysis to determine GTP-bound Rac1. The original extracts were subjected to immunoblot analysis for tubulin, as a loading control.

conditions. To test this hypothesis, first we examined the basal level of activation of ERK/MAPK and Rac1 in cells that were transferred to 1.0% O_2. Fig. 3 B shows that both signaling proteins were activated in 1.0% O_2 or when the cells were treated with 100 μM $CoCl_2$. Because $CoCl_2$ was less effective in activating ERK/MAPK and Rac1, compared with hypoxia, we also assessed the relative abundance of HIF-1α under both sets of conditions and determined that HIF-1α levels were increased more substantially in hypoxia. The extent of Rac1 activation in 1.0% O_2 was statistically significant (1.7 ± 0.2-fold; $P < 0.05$; Fig. 3 C). Higher levels of Rac1 activation were not anticipated, as we analyzed whole cell extracts and Rac1 activation is known to occur locally, at the subcellular level, in the migrating cell (Cho and Klemke, 2002).

uPAR is required for hypoxia-induced EMT

To test whether uPAR is responsible for the increase in cell migration observed in hypoxia, we treated MDA-MB-468 cells with antibodies that block uPA binding to uPAR and inhibit uPAR-initiated cell signaling (Jo et al., 2007). Fig. 4 A shows that the antibodies inhibited the increase in cell migration observed in hypoxia by 90 ± 7% ($P < 0.005$; $n = 6$) without affecting cell migration in 21% O_2. Next, we applied a gene silencing approach. Stable subclones of MDA-MB-468 cells, in which uPAR is silenced, were generated using the pSUPER vector system to express short hairpin (sh) RNA. Two cell lines, sh-uPAR6 and sh-uPAR12 cells, demonstrated 86 ± 2 and 70 ± 9% uPAR knockdown, respectively, as determined by quantitative PCR (qPCR), compared with parental cells that were transfected with empty vector (Fig. 4 B). In 1.0% O_2, the degree of knockdown was 93 ± 1 and 78 ± 2% in sh-uPAR6 and sh-uPAR12 cells, respectively.

Under normoxic conditions, migration of sh-uPAR6 and sh-uPAR12 cells was not significantly affected compared with pSUPER cells; however, when the sh-uPAR6 and sh-uPAR12 cells were transferred to 1.0% O_2, the hypoxia-induced increase in cell migration was inhibited by >70% (Fig. 4 C). In Matrigel invasion experiments performed under normoxic conditions, uPAR gene silencing had a modest effect. sh-uPAR12 cells demonstrated a 47 ± 10% decrease in Matrigel invasion, compared with uPAR-expressing cells ($P < 0.05$; $n = 6$). The decrease in invasion was less pronounced with sh-uPAR6 cells. However, once again, when the experiment was performed in 1.0% O_2, the effects of uPAR gene silencing were more profound. The hypoxia-induced increase in Matrigel invasion was inhibited by >80% in the sh-uPAR6 and sh-uPAR12 cells (Fig. 4 C).

Next, we tested the effects of uPAR gene silencing on Rac1 activation in hypoxia. MDA-MB-468 cells that were transfected with empty vector demonstrated increased Rac1 activation when cultured in 1.0% O_2, as was observed with the parental cells; however, Rac1 was not activated by hypoxia in the sh-uPAR6 and sh-uPAR12 cells (Fig. 4 D). These results support a model in which uPAR plays an essential role in the regulation of Rac1 activation in hypoxia.

To further test the role of uPAR in hypoxia-induced MDA-MB-468 cell EMT, we examined the effects of uPAR gene silencing on cell morphology and E-cadherin immunostaining. When cultured in 1.0% O_2, the control cells, which were transfected with empty vector, adopted a fibroblast-like morphology and demonstrated loss of cell surface E-cadherin, duplicating the changes observed with the parental cells (Fig. 5 A). In contrast, sh-uPAR6 and sh-uPAR12 cells, which were cultured in 1.0% O_2, demonstrated unchanged epithelial cell–like morphology with abundant cell contacts. E-cadherin immunostaining was unchanged (Fig. 5 A).

We also performed studies to compare collagen remodeling by the uPAR-expressing and gene-silenced cells. The three cell lines were plated on coverslips coated with fluorescein-labeled type I collagen. Under normoxic conditions, considerable remodeling of the fluorescent collagen was not observed with any of the cells (Fig. 5 B). In 1.0% O_2, the uPAR-expressing pSUPER cells demonstrated substantial collagen remodeling, as was observed with parental cells. In contrast, the sh-uPAR6 and sh-uPAR-12 cells failed to demonstrate collagen remodeling. Collectively, these results demonstrate that uPAR is required for hypoxia-induced EMT in MDA-MB-468 cells.

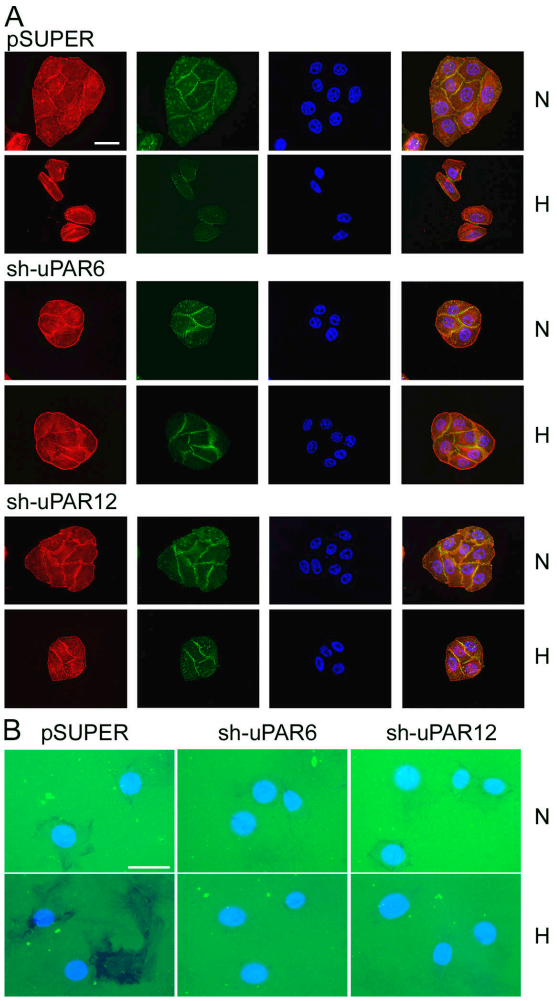

Figure 5. **uPAR is necessary for hypoxia-induced EMT and collagen remodeling.** (A) pSUPER, sh-uPAR6, and sh-uPAR12 cells were cultured for 50 h in 21% O_2 (N) or 1.0% O_2 (H). The preparations were immunostained for E-cadherin (green channel), phalloidin (red channel), and DAPI. (B) pSUPER, sh-uPAR6, and sh-uPAR12 cells were cultured for 18 h on coverslips precoated with fluorescein-labeled type I collagen in 21% O_2 (N) or 1.0% O_2 (H). Cell nuclei are stained with DAPI. Bars, 50 μm.

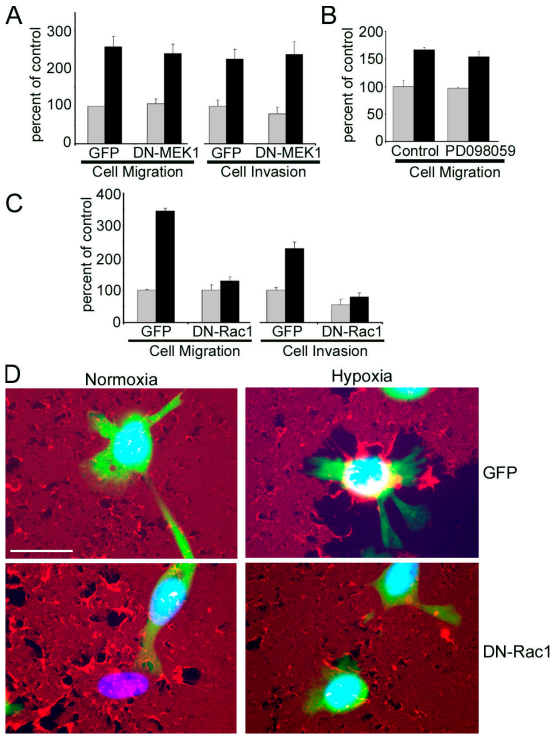

Figure 6. **Rac1 is necessary for hypoxia-induced cell migration, invasion, and collagen remodeling.** (A) MDA-MB-468 cells were transfected to express DN-MEK1 and GFP or GFP alone. Cells were allowed to migrate for 24 h in Transwell chambers (cell migration) or in chambers with reconstituted Matrigel (cell invasion). Experiments were performed in 21% O_2 (gray bars) or 1.0% O_2 (black bars). Migration and invasion are compared with the levels observed with normoxic control cells that expressed GFP (mean ± SEM; $n = 3$). (B) MDA-MB-468 cells were treated with 100 μM $CoCl_2$ (black bars) or with vehicle (gray bars). The same cells also were treated with 50 μM PD098059 or vehicle (control), as indicated. Transwell migration proceeded for 24 h. Cell migration is expressed relative to that observed with cells treated with vehicle (mean ± SEM; $n = 3$). (C) MDA-MB-468 cells were transfected to express DN-Rac1 and GFP or GFP alone. Cells were allowed to migrate for 24 h in Transwell chambers (cell migration) or in chambers with reconstituted Matrigel (cell invasion) in 21% O_2 (gray bars) or 1.0% O_2 (black bars). Results are expressed relative to that observed in normoxic control cells that expressed only GFP (mean ± SEM; $n = 6$). (D) Cells were transfected to express DN-Rac1 and GFP or GFP alone and cultured for 18 h on collagen labeled with Alexa Fluor 594 in 21% O_2 (normoxia) or 1.0% O_2 (hypoxia). Nuclei are stained with DAPI. Bar, 50 μm.

Rac1 is required for MDA-MB-468 cell migration, invasion, and collagen remodeling in hypoxia

Although activation of ERK/MAPK and Rac1 is associated with increased cell migration and with the other properties observed in hypoxic MDA-MB-468 cells, the effects of these cell signaling pathways on cell physiology are cell type specific. Factors that may determine whether activation of ERK/MAPK and/or Rac1 regulate cell migration include but are not limited to the integrin expression pattern of the cell and the composition of the substratum (Anand-Apte et al., 1997; Nguyen et al., 1999). In MCF-7 cells, activation of endogenous EpoR cell signaling in hypoxia promotes cell migration by a pathway that requires ERK/MAPK. Dominant-negative (DN) MEK1 and PD098059 block the response (Lester et al., 2005). However, as shown in Fig. 6 A, in MDA-MB-468 cells, DN-MEK1 failed to inhibit the increase in cell migration induced by hypoxia. Similarly, PD098059 failed to inhibit the increase in cell migration caused by $CoCl_2$ (Fig. 6 B). We also studied the effects of DN-MEK1 expression on Matrigel invasion by MDA-MB-468 cells. Again, no inhibition was observed (Fig. 6 A).

Next, we tested the effects of DN-Rac1 on hypoxia-induced cell migration and invasion. As shown in Fig. 6 C, under normoxic cell culture conditions, DN-Rac1 did not affect cell migration and modestly decreased invasion (45 ± 16%; $P < 0.05$). In contrast, DN-Rac1 almost entirely neutralized the effects of hypoxia on cell migration and Matrigel invasion. We confirmed these results in separate experiments in which we treated cells with 100 μM $CoCl_2$ (instead of hypoxia). DN-Rac1 inhibited the $CoCl_2$-induced increase in cell migration by 87 ± 11% ($P < 0.05$; $n = 3$; unpublished data). We also showed that cells that were transfected to express DN-Rac1 and GFP demonstrate decreased collagen remodeling compared with cells that were transfected to express GFP alone (Fig. 6 D). Thus, DN-Rac1 inhibited changes

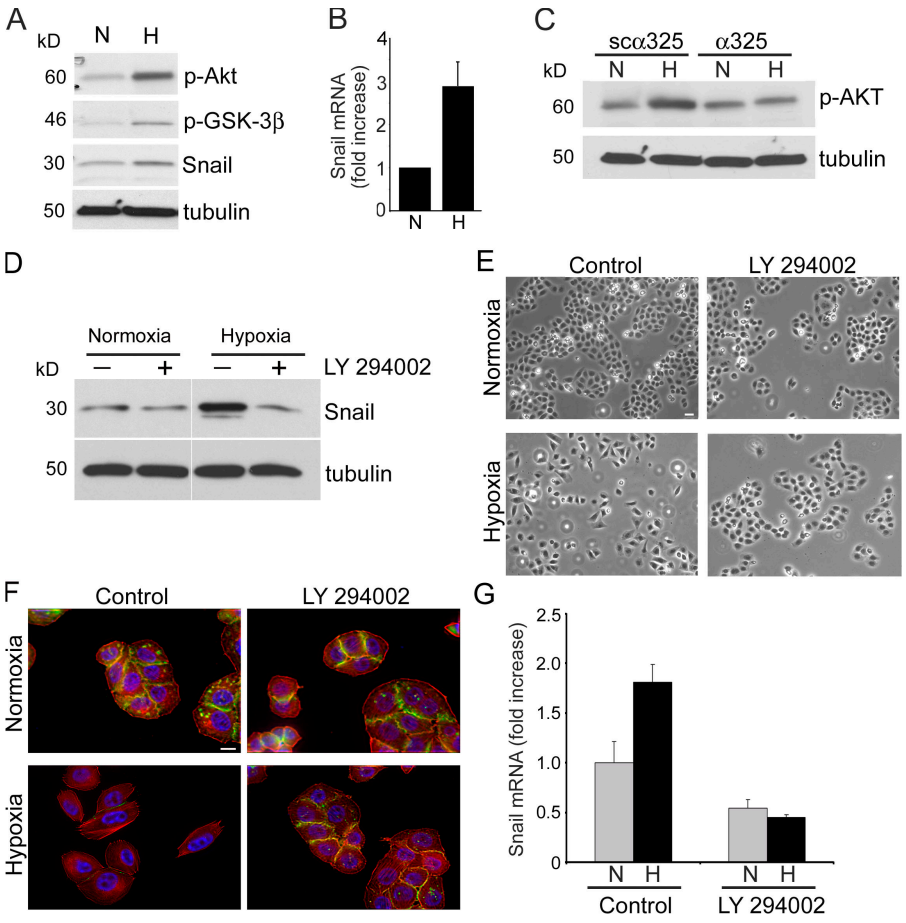

Figure 7. **uPAR-dependent activation of the PI3K–Akt pathway is necessary to induce EMT in hypoxia.** (A and B) MDA-MB-468 cells were cultured for 15 h in 21% O_2 (N) or 1.0% O_2 (H). (A) Cell extracts were subjected to immunoblot analysis to detect phosphorylated Akt (p-Akt), phosphorylated GSK-3β (p-GSK-3β), Snail, and tubulin. (B) Snail mRNA was determined by qPCR (mean ± SEM; $n = 4$). (C) MDA-MB-468 cells were treated with 50 μM synthetic peptide (α325) or 50 μM scrambled peptide (scα325) for 15 h in 21% O_2 (N) or 1.0% O_2 (H). Cell extracts were subjected to immunoblot analysis to detect phosphorylated Akt and tubulin. (D) MDA-MB-468 cells were treated with10 μM of the PI3K inhibitor LY294002 or with vehicle for 15 h in 21% O_2 (normoxia) or 1.0% O_2 (hypoxia). Cell extracts were subjected to immunoblot analysis to detect Snail and tubulin (representative of three studies). All lanes are from the same immunoblot (same exposure). (E–G) MDA-MB-468 cells were treated with 10 μM LY294002 or vehicle (control) and cultured for 50 h in 21% O_2 (normoxia; N) or 1.0% O_2 (hypoxia; H). (E) Cell images were captured using phase-contrast microscopy. (F) Cells were immunostained to detect E-cadherin (green). The same cells were stained with phalloidin (red) and DAPI. (G) Snail mRNA was determined by qPCR. Results are compared with the level observed in control cells in normoxia (mean ± SEM; $n = 3$). Bar, 50 μm.

in three separate functional properties that were associated with EMT in MDA-MB-468 cells under hypoxia.

Phosphatidylinositol 3-kinase (PI3K)–Akt signaling is necessary for uPAR-induced EMT in MDA-MB 468 cells

Diverse cell signaling factors have been implicated in EMT, including Rac1, c-Src, Ras, FAK, and PI3K–Akt (Zhang et al., 2003; Larue and Bellacosa, 2005; Matos and Jordan, 2006). These factors may operate in concert and possibly in a cell-specific manner. Because recent studies indicate that the PI3K–Akt pathway is activated by uPA binding to uPAR (Chandrasekar et al., 2003; Alfano et al., 2006), we explored the role of Akt in hypoxia-induced EMT. As shown in Fig. 7 A, when MDA-MB-468 cells were cultured in 1.0% O_2, the level of phosphorylated Akt (p-Akt) was substantially increased.

In EMT, an important function of Akt is regulation of GSK-3β activity. Akt-induced GSK-3β phosphorylation results in GSK-3β inactivation. Otherwise, GSK-3β stabilizes epithelial cell morphology by targeting Snail. GSK-3β regulates Snail activity by inhibiting Snail expression, promoting Snail degradation, and decreasing nuclear localization (Zhou et al., 2004; Bachelder et al., 2005). Fig. 7 A shows that in hypoxia, the level of phosphorylated GSK-3β in MDA-MB-468 cells was increased. Snail expression also was increased at both the protein and mRNA levels. Snail mRNA was increased 2.9 ± 0.6-fold ($P < 0.05$; $n = 4$) after exposure to 1.0% O_2 for 15 h, as determined by qPCR (Fig. 7 B).

To determine whether uPAR is necessary for Akt activation in hypoxia, we treated MDA-MB-468 cells with synthetic peptide, α325, which disrupts uPAR–integrin interactions and blocks uPAR-initiated cell signaling (Wei et al., 2001; Jo et al., 2007). Fig. 7 C shows that α325 blocked hypoxia-induced Akt phosphorylation. The scrambled version of α325 (scα325) had no effect. Fig. 7 D shows that 10 μM of the PI3K inhibitor, LY294002, blocked the increase in Snail protein level seen in hypoxia. LY294002 also preserved epithelial cell morphology and cell contacts in MDA-MB-468 cells that were exposed to 1.0% O_2 for 50 h, as determined by phase-contrast imaging (Fig. 7 E). Equivalent results were obtained with 5 μM Akt inhibitor (unpublished data). Furthermore, LY294002 preserved cell surface E-cadherin in MDA-MB-468 cells in hypoxia (Fig. 7 F). These results suggest that uPAR-dependent Akt activation is essential for hypoxia-induced EMT. To further test this conclusion, we examined Snail mRNA levels in cells that were treated with LY294002 or vehicle for 50 h. LY294002 decreased Snail mRNA by 45 ± 8% in 21% O_2 and by 75 ± 2% in 1.0% O_2 ($P < 0.05$; $n = 3$), completely neutralizing the effects of hypoxia on Snail mRNA expression (Fig. 7 G).

uPAR overexpression induces EMT in MDA-MB-468 cells in normoxia

Hypoxia activates complex gene expression programs downstream of HIF-1α and other transcription factors (Harris, 2002). Although the data presented thus far indicate that uPAR is

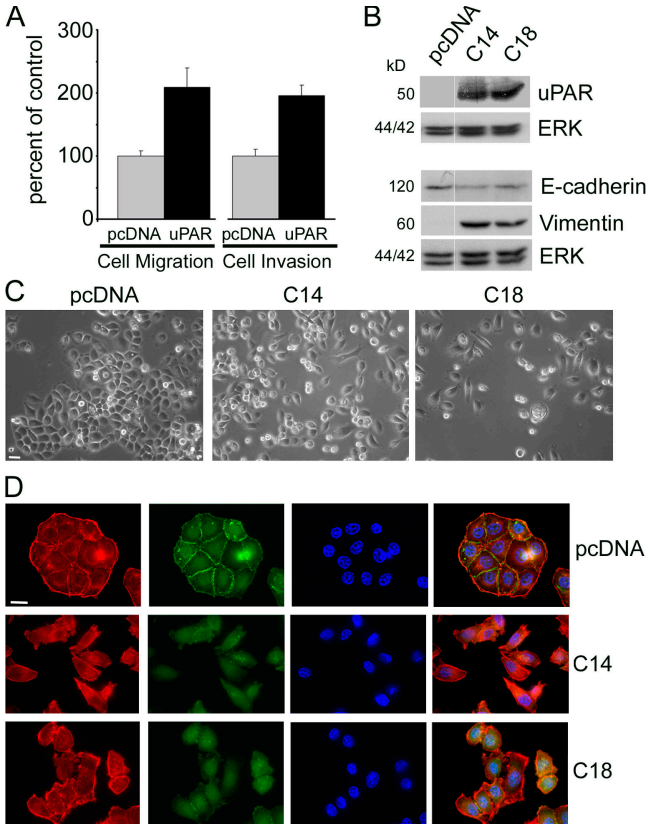

Figure 8. **uPAR overexpression is sufficient to induce EMT under normoxia.** (A) MDA-MB-468 cells were cotransfected to transiently express GFP and uPAR (uPAR) or empty vector (pcDNA). Cells were allowed to migrate in Transwell chambers (cell migration; $n = 9$) or invade Matrigel (cell invasion; $n = 8$) for 24 h. Results are expressed as a percentage of that observed with normoxic GFP-expressing control cells (mean ± SEM). (B) Extracts from cells transfected with empty vector, uPAR-overexpressing C14 cells, and uPAR-overexpressing C18 cells were subjected to immunoblot analysis to detect uPAR and total ERK/MAPK, as a loading control. Equivalent cell extracts were probed to detect E-cadherin, vimentin, and total ERK/MAPK. All lanes are from the same immunoblot (same exposure). (C) pcDNA, C14, and C18 cells were cultured in 21% O_2. Representative images were captured by phase-contrast microscopy. (D) pcDNA, C14, and C18 cells were immunostained to detect E-cadherin (green channel). The same cells also were stained with phalloidin (red channel) and DAPI. Bars, 50 μm.

necessary for EMT in hypoxic MDA-MB-468 cells, we wished to test whether uPAR alone induces EMT in MDA-MB-468 cells. To accomplish this goal, we overexpressed uPAR in MDA-MB-468 cells and studied these cells under normoxic cell culture conditions. Initially, we performed transient transfection experiments, introducing a full-length human uPAR expression construct in pcDNA together with pMAX-GFP, which encodes GFP. Control cells were transfected with pMAX-GFP alone. Migration and Matrigel invasion were studied. Fig. 8 A shows that transient transfection with uPAR increased cell migration by 2.1 ± 0.3-fold ($P < 0.05$; $n = 9$) and Matrigel invasion by 2.0 ± 0.2-fold ($P < 0.005$; $n = 8$).

To examine the effects of uPAR on morphologic and molecular parameters of EMT, stable cell lines that overexpress uPAR were cloned. Fig. 8 B shows two cell lines (C14 and C18) in which uPAR expression was substantially increased. Control cells that were transfected with empty vector (pcDNA) demonstrated equivalent levels of uPAR compared with parental cells; the uPAR is not apparent in the figure because of exposure time. uPAR overexpression in the C14 and C18 cells induced expression of vimentin and decreased E-cadherin expression, as determined by immunoblot analysis (Fig. 8 B). Phase-contrast imaging of the C14 and C18 cells in 21% O_2 (normoxia) revealed loss of cell contacts (Fig. 8 C). Furthermore, in immunofluorescence microscopy studies, E-cadherin was substantially lost from the cell membranes of C14 and C18 cells and localized more diffusely in the cytoplasm (Fig. 8 D). These results indicate that uPAR overexpression independently induces EMT in MDA-MB-468 cells, without exposure to hypoxia.

Hypoxia promotes MDA-MB-468 cell dissemination in vivo

To determine whether hypoxia may promote cancer cell dissemination in vivo, we modified the chicken egg CAM model of Kim et al. (1998). MDA-MB-468 cells were stably transfected to express GFP. To promote tumor growth on the CAMs, the cells were suspended in Matrigel and applied to a 1-cm^2 sterile cotton gauze that was placed on the CAM. Fig. 9 A shows a stereomicroscope image of a tumor that developed after 11 d. The GFP-expressing cells are shown in Fig. 9 B.

To model hypoxia, 25 μl of 100 μM $CoCl_2$ vehicle was applied to the tumor-bearing gauze daily. qPCR studies, performed 4 d after initiating treatment, demonstrated a 3.0 ± 0.7-fold increase in VEGF mRNA expression ($P < 0.05$; $n = 3$) by the $CoCl_2$-treated cells compared with controls (Fig. 9 C). The primers and probes used for these studies were specific for human VEGF. Human uPAR mRNA also was increased 2.6 ± 0.4-fold in the MDA-MB-468 cells that were treated with $CoCl_2$ ($P < 0.01$; $n = 3$). These results suggest that $CoCl_2$ treatment induces changes in MDA-MB-468 cells on CAMs that are equivalent to those observed in cell culture.

To determine whether $CoCl_2$ treatment modifies the propensity of MDA-MB-468 cells to disseminate in vivo, the eggs were killed 11 d after inoculation. The heart–lung block was isolated from each chick embryo, and the number of fluorescent cells or cell clusters was determined by fluorescence microscopy. In chick embryos that were treated with vehicle, the mean number of fluorescent cells/cell clusters detected was 9 ± 2 ($n = 13$; Fig. 9 D). In chick embryos that were treated with $CoCl_2$, the mean was 25 ± 5 ($n = 9$). Thus, $CoCl_2$ treatment induced a 2.7 ± 0.6-fold increase in cancer cell dissemination to the heart–lung block ($P < 0.01$). The complete process of cancer metastasis includes implantation, survival, and growth at the secondary site. Our CAM assays were not designed to assess these latter stages of the metastasis cascade because of the relatively short length of the experiments. Nevertheless, our results still suggest that conditions that model hypoxia in vivo may increase the propensity for cancer cell metastasis.

uPAR expression is increased and EMT induced in multiple cell lines under hypoxia

Increased uPAR expression was previously reported in MDA-MB-231 breast cancer cells under hypoxia (Graham et al., 1999). To test whether uPAR expression is increased in hypoxia

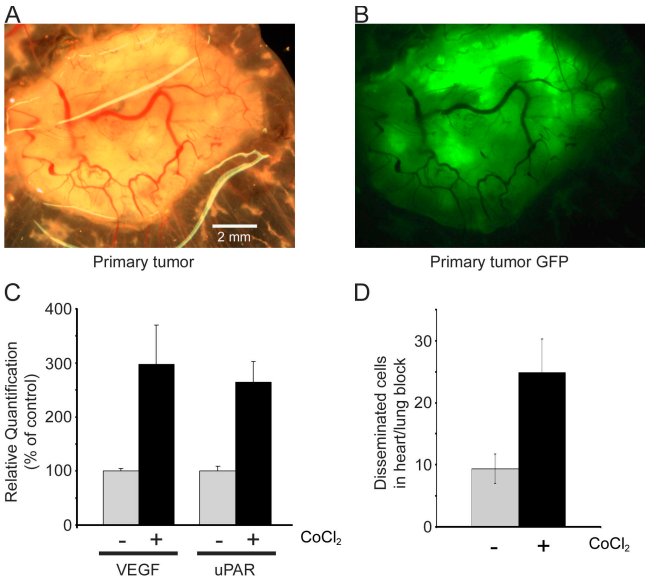

Figure 9. **$CoCl_2$ treatment promotes MDA-MB-468 cancer cell dissemination from CAMs.** GFP-expressing MDA-MB-468 cells were inoculated onto CAMs at 9 d. Tumors were allowed to develop for 11 d. The cells on the CAMs were treated daily with 25 µl of 100 µM $CoCl_2$ (black bars) or vehicle (gray bars). (A) Primary tumors were photographed on a stereomicroscope. (B) GFP-expressing cells were imaged by fluorescence microscopy. (C) Tumors from some eggs were harvested 4 d after inoculation. RNA was isolated and analyzed by qPCR to determine levels of VEGF and uPAR mRNA. mRNA levels were standardized against the levels present in vehicle-treated tumors (mean ± SEM; $n = 3$). (D) Chick embryos were harvested 11 d after inoculation of tumor cells on the CAMs. The number of GFP-expressing cells/cell clusters in the heart–lung block was determined by fluorescent microscopy (mean ± SEM; $n = 9$).

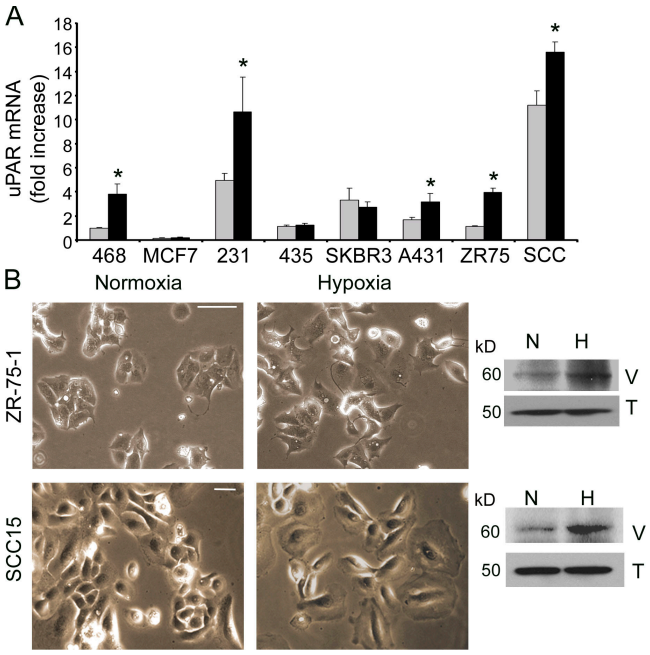

Figure 10. **uPAR expression and EMT in hypoxic cancer cell lines.** (A) MDA-MB-468 (468), MCF-7, MDA-MB-231 (231), MDA-MB-435 (435), SK-BR3, A431, ZR-75-1 (ZR75), and SCC15 (SCC) cells were cultured in 21% O_2 (gray bars) or 1.0% O_2 (black bars). uPAR mRNA was determined by qPCR and standardized against the level present in MDA-MB-468 cells under normoxia (mean ± SEM; $n \geq 3$). *, $P < 0.05$. (B) ZR-75-1 and SCC15 cells were cultured in 21% O_2 (normoxia) or 1.0% O_2 (hypoxia). Images were captured using phase-contrast microscopy. Cell extracts were subjected to immunoblot analysis to detect vimentin (V) and tubulin (T). Bars, 50 µm.

in diverse cancer cells, we screened a series of cell lines by qPCR. Significantly increased uPAR mRNA was observed when MDA-MB-468 cells were cultured in 1.0% O_2 (Fig. 10 A) as anticipated ($P < 0.01$; $n = 5$). MDA-MB-231 cells also demonstrated significantly increased uPAR mRNA in hypoxia ($P < 0.05$; $n = 4$), consistent with the study of Graham et al. (1999). Other cell lines that demonstrated significantly increased uPAR mRNA when exposed to hypoxia included the following: A431 epidermoid carcinoma cells ($P < 0.05$; $n = 3$), ZR-75-1 breast cancer cells ($P < 0.005$; $n = 4$), and SCC15 squamous cell carcinoma cells ($P < 0.05$; $n = 3$). Increased uPAR mRNA was not observed under hypoxic conditions in MDA-MB-435 cells or SK-BR3 cells. MCF-7 cells express extremely low levels of uPAR in 1.0 or 21% O_2, possibly explaining the predominant role of the EpoR in hypoxia in this cell line (Lester et al., 2005). The comparisons shown in Fig. 10 A are accurate to the extent that expression of the housekeeping gene, hypoxanthine phosphoribosyltransferase 1 (HPRT-1), is conserved in the various cells under the conditions of the experiment.

Next, we sought to determine whether EMT is induced in the cells in which uPAR expression is increased in hypoxia. As MDA-MB-231 cells already exhibit a mesenchymal phenotype, we excluded this cell line from our analysis. A431 cells did not demonstrate EMT-associated changes in hypoxia. In contrast, both the ZR-75-1 and SCC15 cells demonstrated phenotypic and molecular changes consistent with EMT. Fig. 10 B shows that the ZR-75-1 cells lost cell contacts and grew more independently in 1.0% O_2. The vimentin level was increased in hypoxia, as determined by immunoblot analysis. The morphology of SCC15 cells in normoxic cell culture was slightly different than that demonstrated by the breast cancer cells, probably because this cancer cell line was derived from squamous cell epithelium, as opposed to columnar epithelium. Again, in 1.0% O_2, cell contacts were lost and the cells grew more independently. Vimentin expression was increased at the protein level, as determined by immunoblot analysis. Thus, hypoxia increased uPAR expression, and this was correlated with EMT-like changes in many, but not all, of the cancer cells studied.

Discussion

Solid tumor growth is limited by the extent of vascularization. Hypoxia generally develops within 100–200 µm from blood vessels (O'Reilly et al., 1996). Without compensatory adaptations, severe hypoxia causes tumor cell death. This is evident in many human cancers and in xenografts, which typically demonstrate large areas of necrosis. Cellular adaptations observed in local hypoxia include changes in cell signaling and gene expression, which promote not only cell survival, but also cell migration, invasion, metastasis, and resistance to chemotherapy (Zhou et al., 2006). Hypoxia-induced changes in cell physiology occur downstream of HIF-1α (Semenza, 2004) and other global transcription factors, such as cAMP regulatory element binding protein (Arany et al., 1996), and are thus polygenic.

Understanding the overall effects of hypoxia on cancer cell physiology is an important goal; however, it is also important to identify individual gene products that may be targeted to counteract the adverse effects of hypoxia in cancer.

In this study, we show that hypoxia induces EMT in breast cancer cells, building on previous studies in which aspects of EMT were reported in hypoxic ovarian carcinoma cells and in renal cell carcinoma (Imai et al., 2003; Krishnamachary et al., 2006). For the first time, we report that uPAR is essential for hypoxia-induced EMT in breast cancer cells. uPAR expression is increased in MDA-MB-468 cells that are cultured in 1.0% O_2, and silencing of uPAR prevents hypoxia-induced EMT. Furthermore, when uPAR is overexpressed in MDA-MB-468 cells, these cells undergo EMT in normoxic cell culture. Zhang et al. (2003) demonstrated EMT in kidney epithelial cells that were transfected to express α3 integrin and uPAR. Our studies extend their work by showing the relationship of uPAR to EMT in cancer cells, by demonstrating the importance of uPAR-dependent cell signaling, and by linking uPAR to EMT in hypoxia.

EMT refers to a series of phenotypic and molecular changes that occur in various steps of normal development and in cancer cells. When EMT occurs in cancer, the prognosis may be adversely affected (Larue and Bellacosa, 2005). Several cell signaling factors have been implicated. Akt may play a central role (Grille et al., 2003; Cheng et al., 2005; Larue and Bellacosa, 2005). A constitutively active mutant of Akt induces EMT in carcinoma cell lines (Grille et al., 2003). Rac1 also has been implicated in EMT. Initially, an alternatively spliced variant of Rac1, called Rac1b, which exists primarily in the GTP-loaded form, was shown to promote EMT in cancer cells (Singh et al., 2004; Radisky et al., 2005); however, there is also evidence that pathways that result in activation of the predominant form of Rac1 may have the same effect (Matos and Jordan, 2006). Other oncogenes, including c-Src and Ras, have been implicated in EMT (Larue and Bellacosa, 2005). Rac1, Akt, c-Src, and Ras are all activated downstream of uPAR (Blasi and Carmeliet, 2002). Thus, we favor a model in which hypoxia-induced uPAR expression activates cell signaling down diverse pathways that are complementary in inducing the full spectrum of cellular changes observed in EMT.

To test our model, we studied two separate uPAR-dependent cell signaling pathways in MDA-MB-468 cells. We showed that Akt is activated in hypoxia and this response is blocked by peptide α325, implicating uPAR (Wei et al., 2001; Jo et al., 2007). The PI3K inhibitor, LY294002, and Akt inhibitor prevented loss of cell contacts in hypoxia. LY294002 also inhibited hypoxia-induced Snail expression and preserved cell surface E-cadherin. These results are best explained by the activity of Akt as a negative regulator of GSK-3β, which controls Snail by suppressing NF-κB–dependent Snail expression, by targeting Snail for degradation, and by inhibiting Snail nuclear localization (Zhou et al., 2004; Bachelder et al., 2005). These GSK-3β activities limit the ability of Snail to function as an E-cadherin transcriptional repressor (Batlle et al., 2000). The linkage of uPAR to Akt activation in hypoxia provides one mechanism by which uPAR may regulate Snail and thus promote EMT. In the same cell culture model system, antagonizing Rac1 blocked the increase in cell migration, Matrigel invasion, and collagen remodeling, which were observed in hypoxia. In our hands, it was not possible to generate stable cultures of DN-Rac1–expressing MDA-MB-468 cells because the cells were not sustainable. Therefore, it was not possible to accurately assess morphologic indices of EMT in cells transfected with DN-Rac1. Nevertheless, our evidence indicates that targeting either Rac1 or the PI3K–Akt pathway blocks cellular properties associated with uPAR-induced EMT in hypoxic breast cancer cells.

Rac1 has emerged as an important cell signaling factor downstream of uPAR in diverse experimental systems (Kjoller and Hall, 2001; Ma et al., 2002; Vial et al., 2003; Wei et al., 2006). uPAR-dependent Rac1 activation does not require uPA, although ERK/MAPK activation by uPA increases uPAR expression (Ma et al., 2001), and this may indirectly lead to an increase in Rac1 activation (Vial et al., 2003). Vitronectin is a provisional ECM protein, which accumulates at sites of inflammation (Schvartz et al., 1999), and thus should be available to activate the uPAR–Rac1 pathway in many malignancies. A recently described pathway in which uPAR supports integrin $\alpha_5\beta_1$ in activating Rac1 (Wei et al., 2006) expands the continuum of contexts in which uPAR may control Rac1 in vivo.

Because hypoxia and $CoCl_2$ promoted breast cancer cell migration and Matrigel invasion in vitro, we wished to study whether hypoxia promotes metastasis in vivo. To accomplish this goal, we established a new model system in which GFP-expressing MDA-MB-468 cells were inoculated onto chicken egg CAMs and treated daily with 100 μM $CoCl_2$. After 11 d, we assessed the number of fluorescent cells/cell clusters in the heart–lung block. We interpreted the presence of cancer cells in the heart–lung block as evidence that the cancer cells had penetrated into the vascular compartment of the chick embryo. In control in vitro experiments, we examined the effects of $CoCl_2$ on MDA-MB-468 cell growth. The $CoCl_2$, at different concentrations, had no effect or was slightly growth inhibitory (unpublished data).

$CoCl_2$ induced changes in MDA-MB-468 cell gene expression on CAMs that were anticipated (increased uPAR and VEGF mRNA). $CoCl_2$ also significantly increased tumor cell dissemination. Thus, we have evidence that the molecular changes that occur in hypoxic breast cancer cells are correlated with an increased propensity for these cells to disseminate in vivo. The increase in cancer cell dissemination may be explained by activation of uPAR-dependent pathways that also result in increased cell migration and Matrigel invasion. However, given that this is a new model system, our results should be interpreted with caution because additional work will be necessary to evaluate the effects of $CoCl_2$ on the CAM surface, which constitutes the tumor cell microenvironment. Possible changes in the microenvironment that could contribute to the increase in cancer cell dissemination include increased vascularization and changes in host cell expression of chemoattractant proteins. Additional studies also will be necessary to confirm the role of uPAR in $CoCl_2$-induced cancer cell dissemination on the CAMs.

In hypoxia, HIF-1α alone may regulate >70 gene products (Semenza, 2004); however, the spectrum of regulated genes is probably cell type specific. In one study, which compared gene

expression in response to HIF-1α in MCF-7 cells and MDA-MB-231 breast cancer cells, 26 genes were up-regulated in both cell types, whereas 63 and 117 genes were up-regulated in only MCF-7 or MDA-MB-231 cells, respectively (Bando et al., 2003). This result may be explained by multiple factors, including but not limited to the karyotype of the cell, gene amplification, post-translational histone modification, CpG methylation, factors that affect transcript stability, and transcription regulatory factors present in the cell before inducing hypoxia (Costello and Plass, 2001; Guhaniyogi and Brewer, 2001; Conley et al., 2006). Cell specificity in the response to hypoxia emerged in our studies when we probed various cell lines for uPAR mRNA expression by qPCR. Our results and prior results reported by others (Graham et al., 1999; Rofstad et al., 2002) indicate that increased uPAR expression may be observed frequently but not uniformly in hypoxia. Therefore, consideration of other receptors, such as the EpoR and c-met, which may be activated in hypoxia (Pennacchietti et al., 2003; Lester et al., 2005), remains important. Although these receptors activate overlapping signaling pathways, the complete activity of each receptor is unique. In ZR-75-1 and SCC15 cells, hypoxia induced significantly increased uPAR mRNA expression and cellular changes consistent with EMT. Thus, the correlation of uPAR expression with EMT in hypoxia was extended beyond the MDA-MB-468 cell system. However, we have not yet determined whether the increase in uPAR expression is responsible for hypoxia-induced EMT in these other two cell lines. Understanding how uPAR and other hypoxia-activated receptors function as regulators of cancer cell physiology in hypoxia remains an important goal.

Materials and methods

Antibodies and reagents

Snail-specific polyclonal antibody and E-cadherin–specific monoclonal antibody (HECD-1) were obtained from Abcam. uPAR-specific antibodies 399R and 3932 and uPA-specific antibody 3471 were obtained from American Diagnostica, Inc. Rac1- and HIF-1α–specific monoclonal antibodies were purchased from BD Biosciences. Rac/Cdc42 assay reagent, which includes residues 67–150 of p21-activated kinase fused to glutathione-*S*-transferase and coupled to glutathione–Sepharose (PAK-1 PBD) was purchased from Millipore. Polyclonal antibody that recognizes total ERK/MAPK was obtained from Millipore. Antibodies that detect phosphorylated ERK/MAPK, phosphorylated Akt, and phosphorylated GSK-3β were obtained from Cell Signaling Technologies. Vimentin-specific monoclonal antibody, tubulin-specific monoclonal antibody, nonspecific murine IgG, and rabbit IgG were obtained from Sigma-Aldrich. The MEK inhibitor, PD098059; the PI3K inhibitor, LY294002; and Akt inhibitor were obtained from EMD Biosciences. Type I collagen was purchased from Southern Biotechnology Associates, Inc. NHS-Fluorescein was obtained from Pierce Chemical Co. The Alexa Fluor 594 protein-labeling kit was obtained from Invitrogen. qPCR reagents, including primers and probes for human uPAR, Snail, VEGF, and HPRT-1 were obtained from Applied Biosystems. Synthetic peptide α325 and its scrambled version, scα325, were obtained from AnaSpec.

The expression construct encoding DN-MEK1 (S217→A) in pBABE was previously described (Catling et al., 1995). pKH3-N17Rac1, which encodes DN-Rac1, was provided by I. Macara (University of Virginia, Charlottesville, VA). The expression construct encoding full-length human uPAR (pcDNA-uPAR) was previously described (Jo et al., 2003). pMAX-GFP, which encodes GFP, was obtained from Amaxa.

Cell culture

MDA-MB-468, MDA-MB-435, ZR-75-1, SCC15, MDA-MB-231, and A431 cells were obtained from American Type Culture Collection. SK-BR3 cells and low-passage MCF-7 cells were provided by S.J. Parsons (University of Virginia, Charlottesville, VA). SK-BR3 cells were cultured in DME (HyClone) supplemented with 10% FBS, 100 U/ml penicillin, and 100 μg/ml streptomycin. MDA-MB-231 cells were cultured in Leibowitz-15 medium (HyClone) with 10% FBS, penicillin, and streptomycin. MCF-7 cells were cultured in RPMI (HyClone) with 10% FBS, penicillin, and streptomycin. SCC15 cells were cultured in a 1:1 mixture of DME/Ham's-F12 with 10% FBS. ZR-75-1 cells were cultured in RPMI with 2 mM L-glutamine, supplemented with 18 mM sodium bicarbonate, 25 mM glucose, 10 mM Hepes, 1.0 mM sodium pyruvate, 10% FBS, penicillin, and streptomycin.

Silencing of uPAR gene expression in MDA-MB-468 breast cancer cells was accomplished using the pSUPER vector system (Oligoengine). The uPAR sequence, AGCCGTTACCTCGAATGCA, corresponding to nucleotides 397–419 of the coding region and fitting the pattern AA(N19)TT with ~50% GC content, was cloned into pSUPER. MDA-MB-468 cells were transfected with this construct or with empty vector using Lipofectamine 2000 (Invitrogen) and selected with 1 μg/ml puromycin. uPAR gene knockdown was assessed by qPCR.

MDA-MB-468 cells that overexpress human uPAR were prepared by transfecting cells with pcDNA-uPAR or with empty vector (pcDNA) using Lipofectamine 2000. After selection for 14 d with 500 μg/ml hygromycin, single-cell clones were established and screened for uPAR expression by immunoblot analysis. GFP-expressing MDA-MB-468 cells were generated by transduction with the lentivirus, pCMV-GIN-Zeo (Open Biosystems), followed by selection with 100 μg/ml zeocin. The brightest 10% of the GFP-expressing cells were selected by FACS and propagated for use in in vivo experiments.

Immunofluorescence microscopy

MDA-MB-468 cells were plated on sterile coverslips. After 18 h, the cells were washed and incubated in serum-free medium under hypoxic (1.0% O_2) or normoxic (21% O_2) conditions for 50 h. Cultures were fixed in 4% formaldehyde, permeabilized with 0.2% Triton X-100, and incubated with antibodies specific for E-cadherin, vimentin, or Snail for 18 h, followed by secondary antibody conjugated with Alexa Fluor 488 and phalloidin conjugated with Alexa Fluor 568 for 1 h (Invitrogen). Control cultures were treated equivalently except for the omission of primary antibody. Preparations were mounted on slides using ProLong Gold with DAPI (Invitrogen) and examined using a fluorescent microscope (DMIRE2; Leica). Images were obtained using a 63× oil-immersion objective (NA 1.4) and a Hamamatsu digital camera with Simple PCI software at room temperature. Deconvolution was performed using Simple PCI software.

Cell migration and invasion assays

Cell migration was studied using 6.5-mm Costar Transwell chambers with 8-μm pores (Corning), as previously described (Nguyen et al., 1998). The Transwell membranes were precoated with 20% FBS on the underside only for 2 h at 37°C. Cells in suspension were treated with 25 μg/ml uPAR-specific antibody 399R, 25 μg/ml uPA-specific antibody, 25 μg/ml nonspecific murine IgG, 25 μg/ml rabbit IgG, 50 μM PD098059, or with vehicle for 15 min before adding the cells to the top chamber (10^5 cells per Transwell). The bottom chamber contained 10% FBS. Cells were allowed to migrate in 21 or 1.0% O_2. In separate studies, the indicated concentration of $CoCl_2$ was added to both chambers. Studies were allowed to proceed for 24 h. At that time, nonmigrating cells were removed from the top surface of each Transwell using a cotton swab. Transwell membranes were then stained with Diff-Quik (Dade-Behring). Cells that migrated through the membrane to the lower surface were counted by light microscopy.

To study the migration of GFP-expressing cells from transiently transfected preparations, translucent Biocoat Cell Culture Inserts (BD Biosciences) were used instead of Transwell membranes. Cells were cotransfected with pMAX-GFP and with constructs encoding DN-MEK, DN-Rac1, or uPAR at a ratio of 1:3. Control cells were transfected with pMAX-GFP and with the empty vector corresponding to each construct. Transmembrane migration was allowed to occur for 24 h. Nonmigrating cells were removed with a cotton swab, and the membranes were fixed in 4% formaldehyde. Cells expressing GFP were counted by fluorescent microscopy.

To study cell invasion, Biocoat Inserts containing reconstituted, growth factor–reduced Matrigel (BD Biosciences) were purchased. Cells that were treated with antibodies or PD098059 and untreated cells were added above the Matrigel matrix. FBS was added to the lower chamber as described for the cell migration experiments. Matrigel invasion was allowed to progress for 24 h in 21 or 1.0% O_2. The Matrigel and cells on the top membrane surface were removed with a cotton swab. Penetration of cells to the underside of the membrane was determined as described for the cell migration experiments.

Collagen remodeling

100 μg/ml type I collagen was adsorbed to glass coverslips by incubation for 24 h at 4°C and labeled with fluorescein or Alexa Fluor 594. MDA-MB-468 cells and subclones thereof were allowed to adhere to the coverslips and cultured for 24 h in 21 or 1.0% O_2. The preparations were fixed in 4% formaldehyde, permeabilized with 0.5% Triton X-100, and mounted on slides using ProLong Gold with DAPI. Images were obtained using a fluorescent microscope (DMIRE2; Leica) on a Hamamatsu digital camera and Simple PCI software.

Immunoblot analysis

MDA-MB-468 cells and subclones thereof were cultured in 60-mm dishes. The cells were transferred to serum-free medium for 6 h and exposed to 1.0% O_2 or 100 μM $CoCl_2$ for 15 h. Control cultures were maintained in 21% O_2. Cell extracts were prepared in ice-cold RIPA buffer (20 mM sodium phosphate, 150 mM NaCl, pH 7.4, 1% NP-40, 0.1% SDS, and 0.5% deoxycholic acid) containing complete protease inhibitor cocktail (Roche) and 1 mM sodium orthovanadate. The protein concentration in each extract was determined by bicinchoninic acid assay (Sigma-Aldrich). Cell extracts were subjected to SDS-PAGE on 10% slabs. Proteins were transferred to polyvinylidene difluoride membranes and probed with antibodies that detect phosphorylated ERK/MAPK, human uPAR, vimentin, phosphorylated Akt, phosphorylated GSK-3β, and snail. The same membranes also were probed to detect tubulin or total ERK/MAPK as a loading control.

Analysis of Rac1 activation

Affinity precipitation of active Rac1 was performed using the fusion protein PAK-1 PBD, which binds specifically to the active, GTP-bound forms of Rac1 and Cdc42 (Azim et al., 2000). MDA-MB-468 and subclones thereof were cultured in 10-cm plates in serum-free medium for 6 h and exposed to 1.0% O_2 or 100 μM $CoCl_2$ for 15 h. Control cultures were maintained in 21% O_2. Cell extracts were prepared in ice-cold RIPA buffer containing protease inhibitor cocktail and 1 mM sodium orthovanadate. The extracts were incubated with 20 μg PAK-1 PBD coupled to glutathione–Sepharose for 60 min at 4°C. The glutathione–Sepharose was washed three times and treated with SDS sample buffer to dissociate the PAK-1 PBD and associated proteins. Cell extracts were subjected to SDS-PAGE on 12% slabs, and immunoblot analysis was performed to detect Rac1. Samples of each cell extract were also subjected to immunoblot analysis before incubation with PAK-1 PBD to determine total Rac1 and tubulin, as a loading control.

qPCR

Total RNA was extracted using the RNeasy kit (QIAGEN). cDNA was synthesized using the iScript cDNA synthesis kit (Bio-Rad Laboratories, Inc.). qPCR was performed using a System 7300 instrument (Applied Biosystems) and a one-step program: 95°C for 10 min, 95°C for 30 s, and 60°C for 1 min, for 40 cycles. HPRT-1 gene expression was measured as a normalizer. Results were analyzed by the relative quantity ($\Delta\Delta C_t$) method. Experiments were performed in triplicate with internal duplicate determinations.

Chicken CAM assay

The original assay for studying tumor metastasis from tumors grown on CAMs (Kim et al., 1998) was modified to facilitate analysis of breast cancer cells. In brief, fertilized white leghorn eggs (McIntyre Farms) were incubated for 9 d before tumor cell inoculation in a rotary incubator at 38°C. GFP-expressing MDA-MB-468 cells were suspended at 4°C in Matrigel at a concentration of 4×10^7 cells/ml. A window was cut in the eggshell above the dropped CAM and a 1.0-cm^2 sterile cotton gauze with a 4-mm^2 center cutout was placed on the membrane. 2×10^6 MDA-MB-468 cells were inoculated onto the CAM through the center of the gauze. To model hypoxia on the CAMs, 25 μl OptiMEM (Invitrogen) medium, with or without 100 μM $CoCl_2$, was applied to the gauze daily for 11 d. Because the gauze was rewet every day, and the tumor was always growing underneath the gauze, we assured saturation of the tumor with $CoCl_2$. At developmental day 20, necropsy was performed on the developing chick embryo. The heart and lungs were isolated, and cell dissemination was quantified under fluorescent microscopy by counting the cells/cell clusters. In parallel experiments, tumors were harvested after 4 d of growth on the CAMs. RNA was isolated and subjected to qPCR analysis to determine levels of human uPAR and VEGF mRNA.

This work was supported by National Institutes of Health grant R01 CA-94900.

Submitted: 17 January 2007
Accepted: 2 July 2007

References

Akakura, N., M. Kobayashi, I. Horiuchi, A. Suzuki, J. Wang, J. Chen, H. Niizeki, K. Kawamura, M. Hosokawa, and M. Asaka. 2001. Constitutive expression of hypoxia-inducible factor-1alpha renders pancreatic cancer cells resistant to apoptosis induced by hypoxia and nutrient deprivation. *Cancer Res.* 61:6548–6554.

Alfano, D., I. Iaccarino, and M.P. Stoppelli. 2006. Urokinase signaling through tts receptor protects against anoikis by increasing BCL-xL expression levels. *J. Biol. Chem.* 281:17758–17767.

Anand-Apte, B., B.R. Zetter, A. Viswanathan, R.-G. Qiu, J. Chen, R. Ruggieri, and M. Symons. 1997. Platelet-derived growth factor and fibronectin-stimulated migration are differentially regulated by the Rac and extracellular signal-regulated kinase pathways. *J. Biol. Chem.* 272:30688–30692.

Andreasen, P.A., L. Kjøller, L. Christenson, and M.J. Duffy. 1997. The urokinase-type plasminogen activator system in cancer metastasis: a review. *Int. J. Cancer.* 72:1–22.

Arany, Z., L.E. Huang, R. Eckner, S. Bhattacharya, C. Jiang, M.A. Goldberg, H.F. Bunn, and D.M. Livingston. 1996. An essential role for p300/CBP in the cellular response to hypoxia. *Proc. Natl. Acad. Sci. USA.* 93:12969–12973.

Azim, A.C., K.L. Barkalow, and J.H. Hartwig. 2000. Determination of GTP loading on Rac and Cdc42 in platelets and fibroblasts. *Methods Enzymol.* 325:257–263.

Bachelder, R.E., S.-O. Yoon, C. Franci, A.G. de Herreros, and A.M. Mercurio. 2005. Glycogen synthase kinase-3 is an endogenous inhibitor of Snail transcription: implications for the epithelial-mesenchymal transition. *J. Cell Biol.* 168:29–33.

Bando, H., M. Toi, K. Kitada, and M. Koike. 2003. Genes commonly upregulated by hypoxia in human breast cancer cells MCF-7 and MDA-MB-231. *Biomed. Pharmacother.* 57:333–340.

Batlle, E., E. Sancho, C. Franci, D. Dominguez, M. Monfar, J. Baulida, and A. Garcia De Herreros. 2000. The transcription factor snail is a repressor of E-cadherin gene expression in epithelial tumour cells. *Nat. Cell Biol.* 2:84–89.

Bianchi, E., R.L. Cohen, A.T. Thor, R.F. Todd III, I.F. Mizukami, D.A. Lawrence, B.M. Ljung, M.A. Shuman, and H.S. Smith. 1994. The urokinase receptor is expressed in invasive breast cancer but not in normal breast tissue. *Cancer Res.* 54:861–866.

Blasi, F., and P. Carmeliet. 2002. uPAR: a versatile signalling orchestrator. *Nat. Rev. Mol. Cell Biol.* 3:932–943.

Cano, A., M.A. Perez-Moreno, I. Rodrigo, A. Locascio, M.J. Blanco, M.G. del Barrio, F. Portillo, and M.A. Nieto. 2000. The transcription factor snail controls epithelial-mesenchymal transitions by repressing E-cadherin expression. *Nat. Cell Biol.* 2:76–83.

Catling, A.D., H.J. Schaeffer, C.W. Reuter, G.R. Reddy, and M.J. Weber. 1995. A proline-rich sequence unique to MEK1 and MEK2 is required for raf binding and regulates MEK function. *Mol. Cell. Biol.* 15:5214–5225.

Chandrasekar, N., S. Mohanam, M. Gujrati, W.C. Olivero, D.H. Dinh, and J.S. Rao. 2003. Downregulation of uPA inhibits migration and PI3k/Akt signaling in glioblastoma cells. *Oncogene.* 22:392–400.

Cheng, J.Q., C.W. Lindsley, G.Z. Cheng, H. Yang, and S.V. Nicosia. 2005. The Akt/PKB pathway: molecular target for cancer drug discovery. *Oncogene.* 24:7482–7492.

Chia, S.K., C.C. Wykoff, P.H. Watson, C. Han, R.D. Leek, J. Pastorek, K.C. Gatter, P. Ratcliffe, and A.L. Harris. 2001. Prognostic significance of a novel hypoxia-regulated marker, carbonic anhydrase IX, in invasive breast carcinoma. *J. Clin. Oncol.* 19:3660–3668.

Cho, S.Y., and R.L. Klemke. 2002. Purification of pseudopodia from polarized cells reveals redistribution and activation of Rac through assembly of a CAS/Crk scaffold. *J. Cell Biol.* 156:725–736.

Conley, B.A., J.J. Wright, and S. Kummar. 2006. Targeting epigenetic abnormalities with histone deacetylase inhibitors. *Cancer.* 107:832–840.

Costello, J.F., and C. Plass. 2001. Methylation matters. *J. Med. Genet.* 38:285–303.

de Vries, T.J., P.H. Quax, M. Denijn, K.N. Verrijp, J.H. Verheijen, H.W. Verspaget, U.H. Weidle, D.J. Ruiter, and G.N. van Muijen. 1994. Plasminogen activators, their inhibitors, and urokinase receptor emerge in late stages of melanocytic tumor progression. *Am. J. Pathol.* 144:70–81.

Del Vecchio, S., M.P. Stoppelli, M.V. Carriero, R. Fonti, O. Massa, P.Y. Li, G. Botti, M. Cerra, G. D'Aiuto, G. Esposito, et al. 1993. Human urokinase receptor concentration in malignant and benign breast tumors by in vitro quantitative autoradiography: comparison with urokinase levels. *Cancer Res.* 53:3198–3206.

Forsythe, J.A., B.H. Jiang, N.V. Iyer, F. Agani, S.W. Leung, R.D. Koos, and G.L. Semenza. 1996. Activation of vascular endothelial growth factor gene transcription by hypoxia-inducible factor 1. *Mol. Cell. Biol.* 16:4604–4613.

Graham, C.H., J. Forsdike, C.J. Fitzgerald, and S. Macdonald-Goodfellow. 1999. Hypoxia-mediated stimulation of carcinoma cell invasiveness via upregulation of urokinase receptor expression. *Int. J. Cancer.* 80:617–623.

Grille, S.J., A. Bellacosa, J. Upson, A.J. Klein-Szanto, F. van Roy, W. Lee-Kwon, M. Donowitz, P.N. Tsichlis, and L. Larue. 2003. The protein kinase Akt induces epithelial mesenchymal transition and promotes enhanced motility and invasiveness of squamous cell carcinoma lines. *Cancer Res.* 63:2172–2178.

Grunert, S., M. Jechlinger, and H. Beug. 2003. Diverse cellular and molecular mechanisms contribute to epithelial plasticity and metastasis. *Nat. Rev. Mol. Cell Biol.* 4:657–665.

Guhaniyogi, J., and G. Brewer. 2001. Regulation of mRNA stability in mammalian cells. *Gene.* 265:11–23.

Harris, A.L. 2002. Hypoxia—a key regulatory factor in tumour growth. *Nat. Rev. Cancer.* 2:38–47.

Harrison, L., and K. Blackwell. 2004. Hypoxia and anemia: factors in decreased sensitivity to radiation therapy and chemotherapy? *Oncologist.* 9:31–40.

Hayman, E.G., M.D. Pierschbacher, Y. Ohgren, and E. Ruoslahti. 1983. Serum spreading factor (vitronectin) is present at the cell surface and in tissues. *Proc. Natl. Acad. Sci. USA.* 80:4003–4007.

Imai, T., A. Horiuchi, C. Wang, K. Oka, S. Ohira, T. Nikaido, and I. Konishi. 2003. Hypoxia attenuates the expression of E-cadherin via up-regulation of SNAIL in ovarian carcinoma cells. *Am. J. Pathol.* 163:1437–1447.

Jo, M., K.S. Thomas, D.M. O'Donnell, and S.L. Gonias. 2003. Epidermal growth factor receptor-dependent and -independent cell-signaling pathways originating from the urokinase receptor. *J. Biol. Chem.* 278:1642–1646.

Jo, M., K.S. Thomas, S. Takimoto, A. Gaultier, E.H. Hsieh, R.D. Lester, and S.L. Gonias. 2007. Urokinase receptor primes cells to proliferate in response to epidermal growth factor. *Oncogene.* 26:2585–2594.

Kim, J., W. Yu, K. Kovalski, and L. Ossowski. 1998. Requirement for specific proteases in cancer cell intravasation as revealed by a novel semiquantitative PCR-based assay. *Cell.* 94:353–362.

Kiyan, J., R. Kiyan, H. Haller, and I. Dumler. 2005. Urokinase-induced signaling in human vascular smooth muscle cells is mediated by PDGFR-beta. *EMBO J.* 24:1787–1797.

Kjoller, L., and A. Hall. 2001. Rac mediates cytoskeletal rearrangements and increased cell motility induced by urokinase-type plasminogen activator receptor binding to vitronectin. *J. Cell Biol.* 152:1145–1157.

Krishnamachary, B., S. Berg-Dixon, B. Kelly, F. Agani, D. Feldser, G. Ferreira, N. Iyer, J. LaRusch, B. Pak, P. Taghavi, and G.L. Semenza. 2003. Regulation of colon carcinoma cell invasion by hypoxia-inducible factor 1. *Cancer Res.* 63:1138–1143.

Krishnamachary, B., D. Zagzag, H. Nagasawa, K. Rainey, H. Okuyama, J.H. Baek, and G.L. Semenza. 2006. Hypoxia-inducible factor-1-dependent repression of E-cadherin in von Hippel-Lindau tumor suppressor-null renal cell carcinoma mediated by TCF3, ZFHX1A, and ZFHX1B. *Cancer Res.* 66:2725–2731.

Larue, L., and A. Bellacosa. 2005. Epithelial-mesenchymal transition in development and cancer: role of phosphatidylinositol 3′ kinase/AKT pathways. *Oncogene.* 24:7443–7454.

Lester, R.D., M. Jo, W.M. Campana, and S.L. Gonias. 2005. Erythropoietin promotes MCF-7 breast cancer cell migration by an ERK/mitogen-activated protein kinase-dependent pathway and is primarily responsible for the increase in migration observed in hypoxia. *J. Biol. Chem.* 280:39273–39277.

Leyland-Jones, B. 2003. Breast cancer trial with erythropoietin terminated unexpectedly. *Lancet Oncol.* 4:459–460.

Liu, D., J.A.A. Ghiso, Y. Estrada, and L. Ossowski. 2002. EGFR is a transducer of the urokinase receptor initiated signal that is required for in vivo growth of a human carcinoma. *Cancer Cell.* 1:445–457.

Ma, Z., D.J. Webb, M. Jo, and S.L. Gonias. 2001. Endogenously produced urokinase-type plasminogen activator is a major determinant of the basal level of activated ERK/MAP kinase and prevents apoptosis in MDA-MB-231 breast cancer cells. *J. Cell Sci.* 114:3387–3396.

Ma, Z., K.S. Thomas, D.J. Webb, R. Moravec, A.M. Salicioni, W.M. Mars, and S.L. Gonias. 2002. Regulation of Rac1 activation by the low density lipoprotein receptor-related protein. *J. Cell Biol.* 159:1061–1070.

Matos, P., and P. Jordan. 2006. Rac1, but not Rac1B, stimulates RelB-mediated gene transcription in colorectal cancer cells. *J. Biol. Chem.* 281:13724–13732.

Monaghan-Benson, E., and P.J. McKeown-Longo. 2006. Urokinase-type plasminogen activator receptor regulates a novel pathway of fibronectin matrix assembly requiring Src-dependent transactivation of epidermal growth factor receptor. *J. Biol. Chem.* 281:9450–9459.

Nguyen, D.H., I.M. Hussaini, and S.L. Gonias. 1998. Binding of urokinase-type plasminogen activator to its receptor in MCF-7 cells activates extracellular signal-regulated kinase 1 and 2 which is required for increased cellular motility. *J. Biol. Chem.* 273:8502–8507.

Nguyen, D.H., A.D. Catling, D.J. Webb, M. Sankovic, L.A. Walker, A.V. Somlyo, M.J. Weber, and S.L. Gonias. 1999. Myosin light chain kinase functions downstream of Ras/ERK to promote migration of urokinase-type plasminogen activator-stimulated cells in an integrin-selective manner. *J. Cell Biol.* 146:149–164.

Nieto, M.A. 2002. The Snail superfamily of zinc-finger transcription factors. *Nat. Rev. Mol. Cell Biol.* 3:155–166.

O'Reilly, M.S., L. Holmgren, C. Chen, and J. Folkman. 1996. Angiostatin induces and sustains dormancy of human primary tumors in mice. *Nat. Med.* 2:689–692.

Ossowski, L., and J.A. Aguirre-Ghiso. 2000. Urokinase receptor and integrin partnership: coordination of signaling for cell adhesion, migration and growth. *Curr. Opin. Cell Biol.* 12:613–620.

Pennacchietti, S., P. Michieli, M. Galluzzo, M. Mazzone, S. Giordano, and P.M. Comoglio. 2003. Hypoxia promotes invasive growth by transcriptional activation of the met protooncogene. *Cancer Cell.* 3:347–361.

Radisky, D.C., D.D. Levy, L.E. Littlepage, H. Liu, C.M. Nelson, J.E. Fata, D. Leake, E.L. Godden, D.G. Albertson, M.A. Nieto, et al. 2005. Rac1b and reactive oxygen species mediate MMP-3-induced EMT and genomic instability. *Nature.* 436:123–127.

Resnati, M., I. Pallavicini, J.M. Wang, J. Oppenheim, C.N. Serhan, M. Romano, and F. Blasi. 2002. The fibrinolytic receptor for urokinase activates the G protein-coupled chemotactic receptor FPRL1/LXA4R. *Proc. Natl. Acad. Sci. USA.* 99:1359–1364.

Rofstad, E.K., H. Rasmussen, K. Galappathi, B. Mathiesen, K. Nilsen, and B.A. Graff. 2002. Hypoxia promotes lymph node metastasis in human melanoma xenografts by up-regulating the urokinase-type plasminogen activator receptor. *Cancer Res.* 62:1847–1853.

Schuster, S.J., E.V. Badiavas, P. Costa-Giomi, R. Weinmann, A.J. Erslev, and J. Caro. 1989. Stimulation of erythropoietin gene transcription during hypoxia and cobalt exposure. *Blood.* 73:13–16.

Schvartz, I., D. Seger, and S. Shaltiel. 1999. Vitronectin. *Int. J. Biochem. Cell Biol.* 31:539–544.

Semenza, G.L. 2001. Hypoxia-inducible factor 1: oxygen homeostasis and disease pathophysiology. *Trends Mol. Med.* 7:345–350.

Semenza, G.L. 2004. Hydroxylation of HIF-1: oxygen sensing at the molecular level. *Physiology (Bethesda).* 19:176–182.

Singh, A., A.E. Karnoub, T.R. Palmby, E. Lengyel, J. Sondek, and C.J. Der. 2004. Rac1b, a tumor associated, constitutively active Rac1 splice variant, promotes cellular transformation. *Oncogene.* 23:9369–9380.

Thiery, J.P. 2002. Epithelial-mesenchymal transitions in tumour progression. *Nat. Rev. Cancer.* 2:442–454.

Thompson, E.W., D.F. Newgreen, and D. Tarin. 2005. Carcinoma invasion and metastasis: a role for epithelial-mesenchymal transition? *Cancer Res.* 65:5991–5995.

Vaupel, P., and L. Harrison. 2004. Tumor hypoxia: causative factors, compensatory mechanisms, and cellular response. *Oncologist.* 9:4–9.

Vial, E., E. Sahai, and C.J. Marshall. 2003. ERK-MAPK signaling coordinately regulates activity of Rac1 and RhoA for tumor cell motility. *Cancer Cell.* 4:67–79.

Wang, G.L., and G.L. Semenza. 1993. General involvement of hypoxia-inducible factor 1 in transcriptional response to hypoxia. *Proc. Natl. Acad. Sci. USA.* 90:4304–4308.

Wei, Y., M. Lukashev, D.I. Simon, S.C. Bodary, S. Rosenberg, M.V. Doyle, and H.A. Chapman. 1996. Regulation of integrin function by the urokinase receptor. *Science.* 273:1551–1555.

Wei, Y., J.A. Eble, Z. Wang, J.A. Kreidberg, and H.A. Chapman. 2001. Urokinase receptors promote beta1 integrin function through interactions with integrin alpha3beta1. *Mol. Biol. Cell.* 12:2975–2986.

Wei, Y., C.-H. Tang, Y. Kim, L. Robillard, F. Zhang, M.C. Kugler, and H.A. Chapman. 2006. Urokinase receptors are required for alpha 5beta 1 integrin-mediated signaling in tumor cells. *J. Biol. Chem.* 282:3929–3939.

Zhang, F., C.C. Tom, M.C. Kugler, T.T. Ching, J.A. Kreidberg, Y. Wei, and H.A. Chapman. 2003. Distinct ligand binding sites in integrin alpha3beta1 regulate matrix adhesion and cell-cell contact. *J. Cell Biol.* 163:177–188.

Zhou, B.P., J. Deng, W. Xia, J. Xu, Y.M. Li, M. Gunduz, and M.-C. Hung. 2004. Dual regulation of Snail by GSK-3β-mediated phosphorylation in control of epithelial-mesenchymal transition. *Nat. Cell Biol.* 6:931–940.

Zhou, J., T. Schmid, S. Schnitzer, and B. Brune. 2006. Tumor hypoxia and cancer progression. *Cancer Lett.* 237:10–21.